Cell Reports
Article

ZIP8 Regulates Host Defense through Zinc-Mediated Inhibition of NF-κB

Ming-Jie Liu,[1] Shengying Bao,[1] Marina Gálvez-Peralta,[5] Charlie J. Pyle,[1] Andrew C. Rudawsky,[1] Ryan E. Pavlovicz,[2] David W. Killilea,[6] Chenglong Li,[2,3] Daniel W. Nebert,[5] Mark D. Wewers,[1] and Daren L. Knoell[1,4,*]
[1]Dorothy M. Davis Heart and Lung Research Institute
[2]Biophysics Program
[3]Division of Medicinal Chemistry & Pharmacognosy, College of Pharmacy
[4]Department of Pharmacy
The Ohio State University, Columbus, OH 43210, USA
[5]Department of Environmental Health, and Center for Environmental Genetics, University of Cincinnati Medical Center, Cincinnati, OH 45267, USA
[6]Nutrition and Metabolism Center, Children's Hospital Oakland Research Institute, Oakland, CA 94609, USA
*Correspondence: daren.knoell@osumc.edu
http://dx.doi.org/10.1016/j.celrep.2013.01.009

SUMMARY

Activation of the transcription factor NF-κB is essential for innate immune function and requires strict regulation. The micronutrient zinc modulates proper host defense, and zinc deficiency is associated with elevated inflammation and worse outcomes in response to bacterial infection and sepsis. Previous studies suggest that zinc may regulate NF-κB activity during innate immune activation, but a mechanistic basis to support this has been lacking. Herein, we report that the zinc transporter SLC39A8 (ZIP8) is a transcriptional target of NF-κB and functions to negatively regulate proinflammatory responses through zinc-mediated down-modulation of IκB kinase (IKK) activity in vitro. Accordingly, fetal fibroblasts obtained from *Slc39a8* hypomorphic mice exhibited dysregulated zinc uptake and increased NF-κB activation. Consistent with this, mice provided zinc-deficient dietary intakes developed excessive inflammation to polymicrobial sepsis in conjunction with insufficient control of IKK. Our findings identify a negative feedback loop that directly regulates innate immune function through coordination of zinc metabolism.

INTRODUCTION

The innate immune system constitutes the front line of host defense by triggering inflammation, a primordial response designed to protect the host against pathogen invasion (Takeuchi and Akira, 2010). Upon recognition of pathogen-associated molecular patterns, the Toll-like receptor (TLR) pathway becomes activated in immune cells that include monocytes, macrophages, dendritic cells, and nonprofessional cells such as lung epithelia (Kawai and Akira, 2010). Inflammatory mediators are then rapidly released to further alert the remainder of the immune system. TLR signaling initiates recruitment of adaptor molecules such as TRIF, TIRAP, and MyD88 (Takeuchi and Akira, 2010). In turn, the danger signal is transmitted coordinately through a series of molecular events that involve the IRAK family, TRAF6, and TAK1, leading to activation of IκB kinase (IKK) and mitogen-activated protein kinases (MAPKs) (Hayden and Ghosh, 2008; Johnson and Lapadat, 2002). Activation of the IKK complex, which includes IKKα, IKKβ, and NEMO, results in IκB phosphorylation and degradation, thereby allowing phosphorylated NF-κB dimers to translocate into the nucleus and bind κB sites located within target gene promoters for the activation of transcription (Hayden and Ghosh, 2008). Simultaneously, activation of MAPKs upregulates ERKs, JNKs, and p38, leading to the activation of the transcriptional factor AP-1 (Johnson and Lapadat, 2002). IKKβ can also activate ERKs through crosstalk (Tpl2-MEK1/2) between the NF-κB and MAPKs/AP-1 pathways (Banerjee et al., 2006; Waterfield et al., 2004).

Coordination of the initial host response to infection through regulation of the NF-κB and MAPK pathways must be tightly regulated in order to maintain proper immune balance, thereby maximizing host defense while simultaneously minimizing collateral damage (Liew et al., 2005). In order to achieve precise balance, multiple counterregulatory elements have evolved within these pathways that include but are not limited to IκBα (Chiao et al., 1994), MyD88s (Burns et al., 2003), IRAKM (Kobayashi et al., 2002), A20 (Boone et al., 2004), and NLRC5 (Cui et al., 2010). The expression and function of many of these negative regulators including IκBα, A20, MyD88s, and IRAKM are themselves activated by TLR ligands and thus constitute classic negative regulatory feedback loops that ensure attenuation of the TLR response in a threshold-dependent manner (Ruland, 2011).

Sepsis is the leading cause of death in critically ill patients in the United States (Angus et al., 2001), and its incidence has increased over the past two decades (Martin et al., 2003). A major cause of sepsis-related morbidity and mortality is overwhelming inflammation, referred to as the "cytokine storm," driven by the excessive production of inflammatory mediators

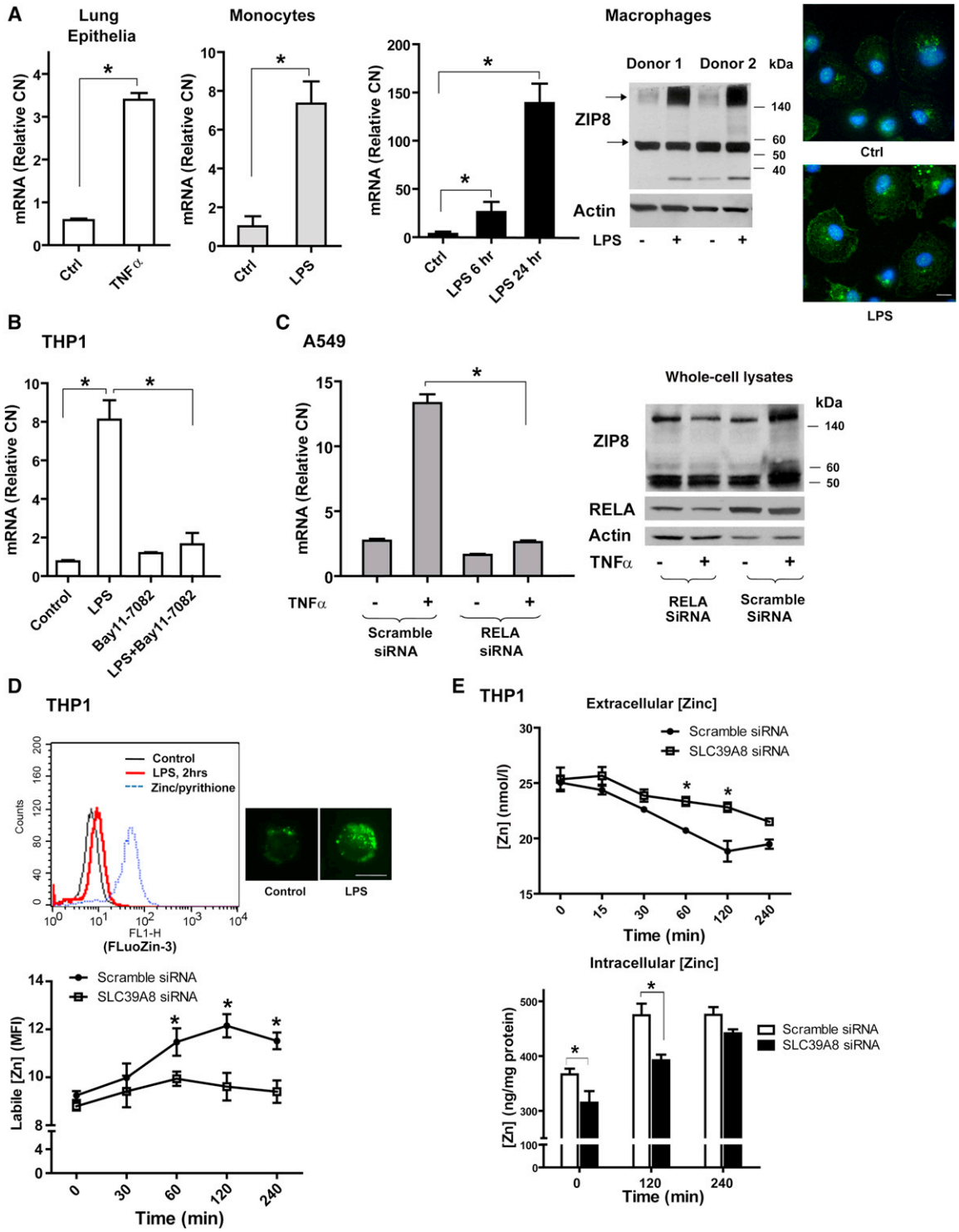

Figure 1. *SLC39A8* Expression Is Induced by Proinflammatory Stimuli in an NF-κB-Dependent Manner and Regulates Zinc Uptake

(A) Human primary lung epithelia were treated with TNF-α (10 ng/ml) for 16 hr (n = 3), human primary monocytes were treated with LPS (1 μg/ml) for 4 hr (n = 4), and CD14+ monocyte-derived primary macrophages were treated with LPS (1 μg/ml) for 6 and 24 hr. SLC39A8 mRNA levels were determined by real-time PCR analysis. Relative CN, RCN. Western blot was performed on membrane fractions with ZIP8 antiserum. Immunofluorescence staining shows ZIP8 localization (green) in macrophages, counterstained with DAPI (scale bar, 10 μm). Ctrl, control.

(B) THP1 cells were treated with LPS (1 μg/ml) for 4 hr with Bay11-7082 (20 μM), added 30 min prior to LPS.

(C) A549 cells were treated with TNF-α (10 ng/ml) in combination with RELA siRNA (40 pmol), which was transfected 24 hr before TNF-α treatment.

(legend continued on next page)

within hours of pathogen invasion (Hotchkiss and Karl, 2003; Warren, 1997). The magnitude of the innate immune response to infection directs the cumulative host response with respect to tissue injury and survival (Abraham and Singer, 2007). Importantly, patients with sepsis who encounter an exaggerated initial inflammatory response are more susceptible to tissue injury and mortality, but it remains unclear why or how this occurs (Parrillo, 1993).

Zinc, an essential trace element, facilitates the coordination of innate and adaptive immunity (Rink and Haase, 2007). Zinc deficiency causes immune dysfunction resulting in increased morbidity and mortality following infection (Caulfield et al., 2004), whereas zinc supplementation prevents the incidence of infectious diseases and improves immune function (Brooks et al., 2005; Prasad et al., 2007). Zinc metabolism is primarily coordinated by zinc transporters. In mammals, these transmembrane-spanning proteins are encoded by two solute-linked carrier (SLC) gene families that include 14 SLC39 (also known as ZIP) family members and 10 SLC30 (aka ZnT) family members. SLC39 transporters increase cytosolic zinc content by promoting extracellular uptake or release from subcellular organelles, whereas SLC30 transporters function as counterregulators that decrease intracellular zinc levels (Lichten and Cousins, 2009).

Despite recent advances (Aydemir et al., 2009; Kitamura et al., 2006; Nishida et al., 2009; Yu et al., 2011), much remains unknown regarding the influence of zinc transporters on zinc metabolism relative to innate immunity (Lichten and Cousins, 2009). Zinc metabolism changes rapidly in response to systemic infection in humans, leading to rapid mobilization of intravascular zinc into vital organs with a consequent decrease in circulating plasma zinc levels (hypozincemia) (Cousins and Leinart, 1988; Gaetke et al., 1997; Sobocinski et al., 1978). Zinc redistribution is primarily driven by induction of key zinc transporters, as exemplified by the upregulation of Slc39a14 (ZIP14) mediated by IL-6 (Liuzzi et al., 2005). Importantly, lower-than-expected circulating zinc levels correlate with higher mortality in humans with sepsis (Wong et al., 2007), although the consequences of altered zinc metabolism in this setting are not yet known.

Using a mouse model of polymicrobial sepsis, we reported that zinc deficiency increases systemic inflammation and mortality, whereas zinc supplementation suppresses inflammation and improves survival, suggesting that zinc metabolism plays an important regulatory role during the early stage of sepsis (Bao et al., 2010; Knoell et al., 2009). Our group and others have identified SLC39A8 (ZIP8) as the most significantly upregulated transporter in response to cytokines, bacteria, and sepsis, suggesting its unique role in innate immune function (Begum et al., 2002; Besecker et al., 2008; Besecker et al., 2011). Herein, we report that ZIP8 is a negative feedback regulator of NF-κB and innate immune activation in response to infection through coordination of zinc metabolism. These findings help to bridge an existing gap in our fundamental understanding of how zinc affects innate immunity and host defense.

RESULTS

Proinflammatory Stimuli Induce *SLC39A8* Expression in an NF-κB-Dependent Manner, Resulting in Zinc Influx

SLC39A8 expression is upregulated in primary human lung epithelia, monocytes, and macrophages in response to TNF-α or lipopolysaccharide (LPS). SLC39A8 (ZIP8) protein localizes mainly to the plasma membrane, in addition to lysosomal or mitochondrial membranes (Aydemir et al., 2009; Besecker et al., 2008). ZIP8 is heavily glycosylated following stimulation, leading to increased expression of a high molecular weight, membrane-associated protein (Figures 1A, and Figures S1A, and S1B), suggesting that additional posttranscriptional (or translational) regulatory events are at play in controlling protein function (that will require further study). Mouse Slc39a8 possesses 89% amino acid sequence and 96% ZIP domain sequence identity with human SLC39A8, implying a high degree of conservation (Girijashanker et al., 2008). As expected, LPS also induced *Slc39a8* expression in mouse RAW 267.4 cells (Figure S1C). We next examined whether *SLC39A8* expression is NF-κB dependent. Suppression of NF-κB by pharmacologic inhibition or *RELA*-specific siRNA significantly inhibited *SLC39A8* expression induced by LPS or TNF-α (Figures 1B and 1C).

Because ZIP8 is a zinc importer, we then determined whether changes in ZIP8 expression result in changes in intracellular zinc content. Using the cell-permeable zinc indicator FluoZin-3, we revealed that intracellular labile zinc levels rapidly increased in response to LPS but was significantly impaired in ZIP8-silenced cells (Figure 1D), indicating that ZIP8 plays an important role in regulating zinc uptake shortly following TLR activation. The representative pictures depict the unique pattern of intracellular labile zinc. We further observed a decrease in total zinc content in the culture medium with a corresponding increase within cells, establishing that elevation of intracellular labile zinc content occurs following transport across the plasma membrane via ZIP8 (Figure 1E). As expected, we also observed a significant increase in intracellular labile zinc levels when ZIP8 was overexpressed (Figure S1D).

SLC39A8 Transcription Is Directly Regulated by NF-κB

Inspection of the human *SLC39A8* gene sequence revealed four potential transcript variants, indicating that its transcription may be initiated at multiple transcriptional start sites (TSSs). Based on this, 5′RACE (rapid amplification of cDNA ends) was conducted and revealed two TSSs, but only one was induced by TNF-α (Figures S2A–S2C). The inducible TSS was in close proximity to the known TSS of the reference sequence (NM_022154.5). Based upon their close proximity, the known TSS served as the basis of subsequent studies (Aiba et al., 2008).

(D) Control siRNA or SLC39A8 siRNA-treated THP1 cells were stimulated with LPS (1 μg/ml), followed by FluoZin-3 staining. Intracellular labile zinc was quantified by flow cytometry. MFI, mean fluorescence intensity. Representative composite flow cytometric histograms are shown, and $ZnSO_4$ (10 μM)/pyrithione (10 μM) served as a positive control. Two representative FluoZin-3 staining images are shown (scale bar, 10 μm). Western analysis of ZIP8 silencing is shown in Figure 3A.
(E) Total zinc levels in culture medium and cell pellets were detected by AAS or ICP-OES, respectively.
Data are presented as mean ± SD. *$p < 0.05$. See also Figure S1.

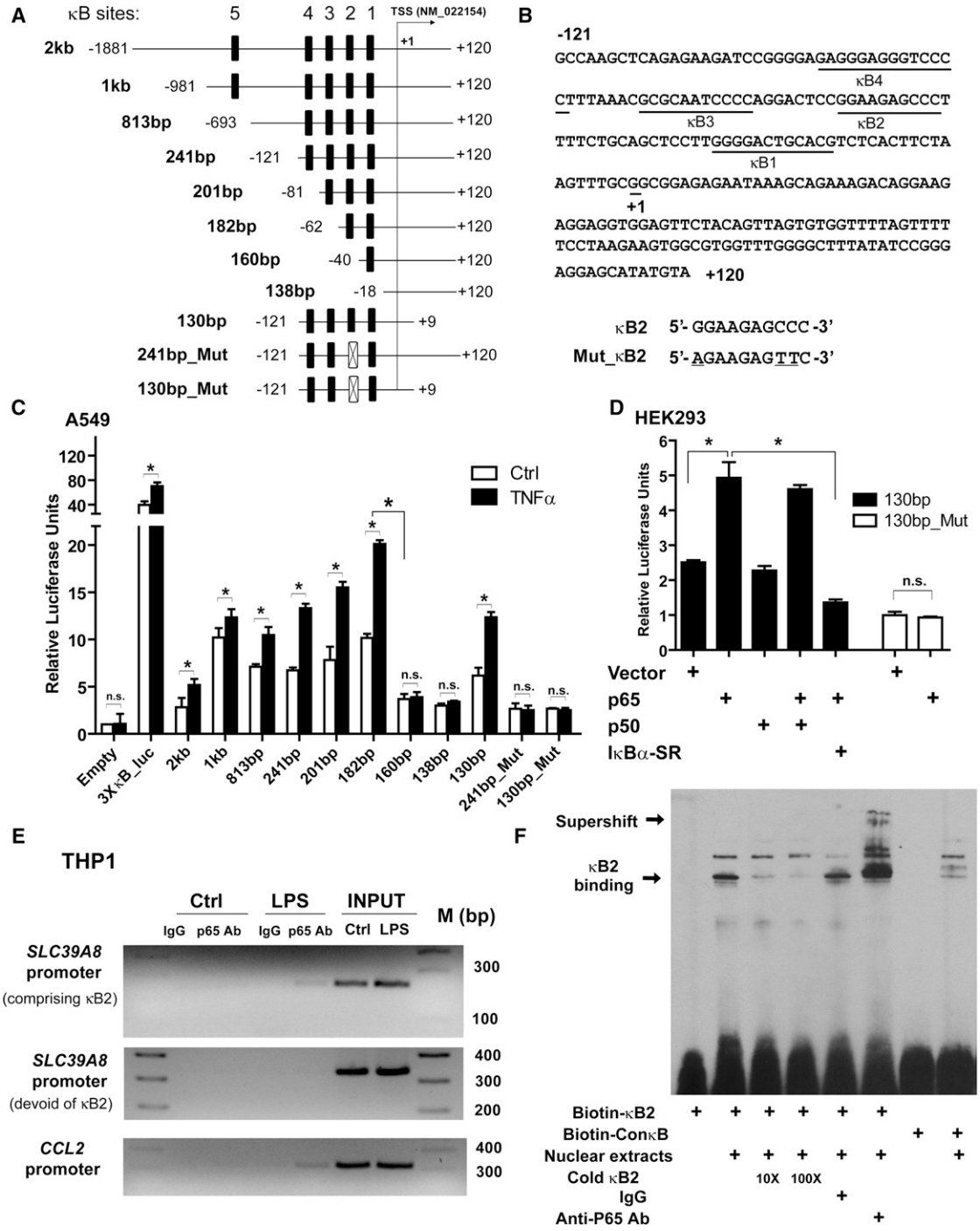

Figure 2. Transcriptional Activation of the Human *SLC39A8* Promoter by NF-κB

(A) Schematic diagram depicts a 2 kb *SLC39A8* promoter region and its serial deletion constructs that were cloned into a pGL3-Basic vector.

(B) Sequence of the key promoter region and four potential putative NF-κB-binding sites.

(C) Constructs were transfected into A549 cells, followed by TNF-α (10 ng/ml) treatment for 24 hr. Serial deletion identified κB2 as the critical binding site. The NF-κB reporter 3 × κB-luc served as the positive control. Site-directed mutagenesis of the κB2 site resulted in the loss of promoter activity.

(D) Ectopic expression of p65, but not p50, induced promoter activity of the 130 bp construct, which was further inhibited by IκBα-SR. Moreover, a mutated construct (130-bp_Mut) was not responsive to p65.

(E) ChIP-based PCR analysis of p65-bound chromatin DNA, which was immunoprecipitated from THP1 cells treated with vehicle or LPS (1 μg/ml) for 1 hr. A 234 bp band containing κB2 was amplified from the *SLC39A8* promoter region. The adjacent region devoid of κB2 was amplified as a negative control. *CCL2* served as a positive control.

(legend continued on next page)

NF-κB activates gene transcription following physical interaction with the κB-binding motif located within the regulatory region of target genes. Analysis of the human *SLC39A8* gene (Match) revealed five potential putative κB-binding sites in the 5′-flanking region (Figure 2A). The sequences of κB 1–4 are shown in Figure 2B. To determine whether the κB sites are transcriptionally active, a 2 kb promoter fragment (−1,881 to +120) of human genomic DNA was amplified and cloned into a pGL3 luciferase reporter. A series of plasmids with progressively truncated promoter regions were subsequently developed and used to locate a 100 bp region proximal to the TSS, containing κB 1–4, which was required for promoter activity (Figures 2A and 2C). Serial deletion of κB regions 1–4 identified κB2 as the critical binding site. Loss of κB2 resulted in a decrease of both constitutive and inducible activity (Figures 2C and S2D). Ectopic expression of p65 also induced κB2-mediated expression, whereas the IκBα superrepressor (SR) inhibited induction (Figure 2D). Confirmation of the κB2 site was achieved by site-directed mutagenesis (Figures 2C and 2D). Chromatin immunoprecipitation (ChIP) analysis demonstrated in vivo binding of NF-κB p65 to the *SLC39A8* promoter region, and EMSA analysis revealed physical binding of κB2 oligonucleotides with activated NF-κB (p65) in vitro (Figures 2E, 2F, S2E, and S2F).

ZIP8 Is a Potent Negative Regulator of NF-κB Activation

Transcriptional induction of ZIP8 by NF-κB revealed that ZIP8 may assist in coordination of host defense. We first determined the extent of immune activation following ZIP8 knockdown in human monocytes and lung epithelia. Under all conditions studied, suppression of ZIP8 expression resulted in increased production of proinflammatory mediators (cytokines) (Figures 3A, 3B, S3A, S3B, and S3E). Consistent with this, endogenous NF-κB-binding activity was higher when ZIP8 expression was silenced in THP1 cells (Figure S3D). We then screened signaling effectors of the NF-κB and MAPK pathways (Figures 3C and S3C). Suppression of ZIP8 expression increased phosphorylation of p65 and IκBα, two known substrates of IKKβ, suggesting that ZIP8 affects the activity of the IKK complex. An increase in p-ERK, p-Akt, and A20 levels was also observed. The minor change observed in phosphorylation of IKKα/β indicated that ZIP8 suppression did not significantly impact the activity of IKK upstream signaling intermediates. Consistent with this, IRAK1 was degraded with similar kinetics in both control and ZIP8-silenced cells. No appreciable differences in JNK phosphorylation were observed. We then immunoprecipitated the IKK complex and directly measured its activity. Suppression of ZIP8 significantly increased IKK activity in response to LPS, thereby providing evidence that ZIP8-mediated effects occur at or proximal to IKK (Figure 3D). Consistent with its role as a negative regulator, we observed that overexpression of ZIP8 inhibits NF-κB activation induced by TNF-α or IL-1β (Figures 3E and S3F). Knowing that overexpression of MyD88, TRAF6, IKKβ, or p65 induces NF-κB (Cui et al., 2010), we cotransfected ZIP8 with each signaling molecule and found that overexpression of ZIP8 with either MyD88, TRAF6 or IKKβ, but not p65, inhibited NF-κB activation, indicating that the location of the ZIP8 effect is at or upstream of IKKβ (Figures 3F and S3G). Taken together, these findings strongly indicate that ZIP8 negatively regulates NF-κB through down-modulation of IKK. Additionally, we observed that augmentation of NF-κB activation by ZIP8 knockdown was reduced by the addition of zinc in combination with pyrithione, an ionophore that facilitates zinc entry into the cytosol (Figure 3G). This observation led us to then determine whether the negative regulatory impact of ZIP8 on NF-κB is dependent on zinc.

Zinc Suppresses NF-κB Activation through Direct Interaction with IKK

Zinc is known to inhibit NF-κB activation, but the underlying mechanism remains unclear (Haase and Rink, 2009; Jeon et al., 2000). We observed that zinc significantly inhibited the expression of NF-κB-dependent transcripts or luciferase reporter (Figures S4A and S4B). The phosphorylation of IκBα was markedly inhibited, and degradation of IκBα was nearly abolished, resulting in a significant reduction in p65 nuclear translocation. A significant time-dependent inhibition of IKK activity was also observed (Figure 4A). Meanwhile, zinc was not found to inhibit the activity of the E3 ligase $SCF^{\beta\text{-TrCP}}$ complex that mediates IκBα ubiquitination and degradation (data not shown). We also observed that zinc inhibited NF-κB activity driven by overexpression of MyD88, TRAF6, and IKKβ, but not p65, mapping the location of the effect at IKK, identical to our previous findings involving ZIP8 cotransfection (Figure S4B). Given the remarkable similarity between ZIP8- and zinc-mediated effects that identified IKK complex as the target, we next determined whether zinc directly binds to and inhibits IKK. First, we observed that recombinant IKKα or IKKβ was directly inhibited by zinc in a dose-responsive manner (IC_{50} for IKKα: 0.52 μM [95% CI 0.42–0.64 μM]; IC_{50} for IKKβ: 0.43 μM [95% CI, 0.32–0.58 μM]) (Figure 4B). To understand whether zinc selectively inhibits IKKα and/or IKKβ, we exposed $IKK\beta^{(-/-)}$ mouse embryonic fibroblasts (MEFs) to IL-1β and evaluated NF-κB-mediated function. As expected, $IKK\beta^{(-/-)}$ cultures exhibited impaired NF-κB activation and were less responsive to IL-1β when compared to $IKK\beta^{(+/+)}$ cultures (Li et al., 1999). In particular, zinc/pyrithione inhibited IκBα phosphorylation and degradation as well as IL-6 production in $IKK\beta^{(+/+)}$ cells, whereas these effects were attenuated in $IKK\beta^{(-/-)}$ cultures (Figures 4C and S4C). Although recombinant IKKα was inhibited by zinc, $IKK\beta^{(-/-)}$ MEFs that contain IKKα did not exhibit zinc-mediated inhibition, indicating that the primary effect of zinc occurs directly through inhibition of IKKβ and/or IKKβ-related kinase complex formation. We also conducted similar experiments in $NEMO^{(-/-)}$ MEFs but did not observe zinc-mediated effects because cultures were completely unresponsive to proinflammatory cytokines (data not shown) (Rudolph et al., 2000).

(F) EMSA revealed the binding of biotin-labeled κB2 with nuclear extracts from TNF-α-treated A549 cells. Binding was inhibited by an excess of unlabeled κB2 oligonucleotides (10 × and 100 ×). Coincubation with a p65 antibody produced a supershift. The biotin-labeled NF-κB consensus sequence (ConκB) served as a positive control.

Data are presented as mean ± SD. *$p < 0.05$; n.s., not significantly different. See also Figure S2.

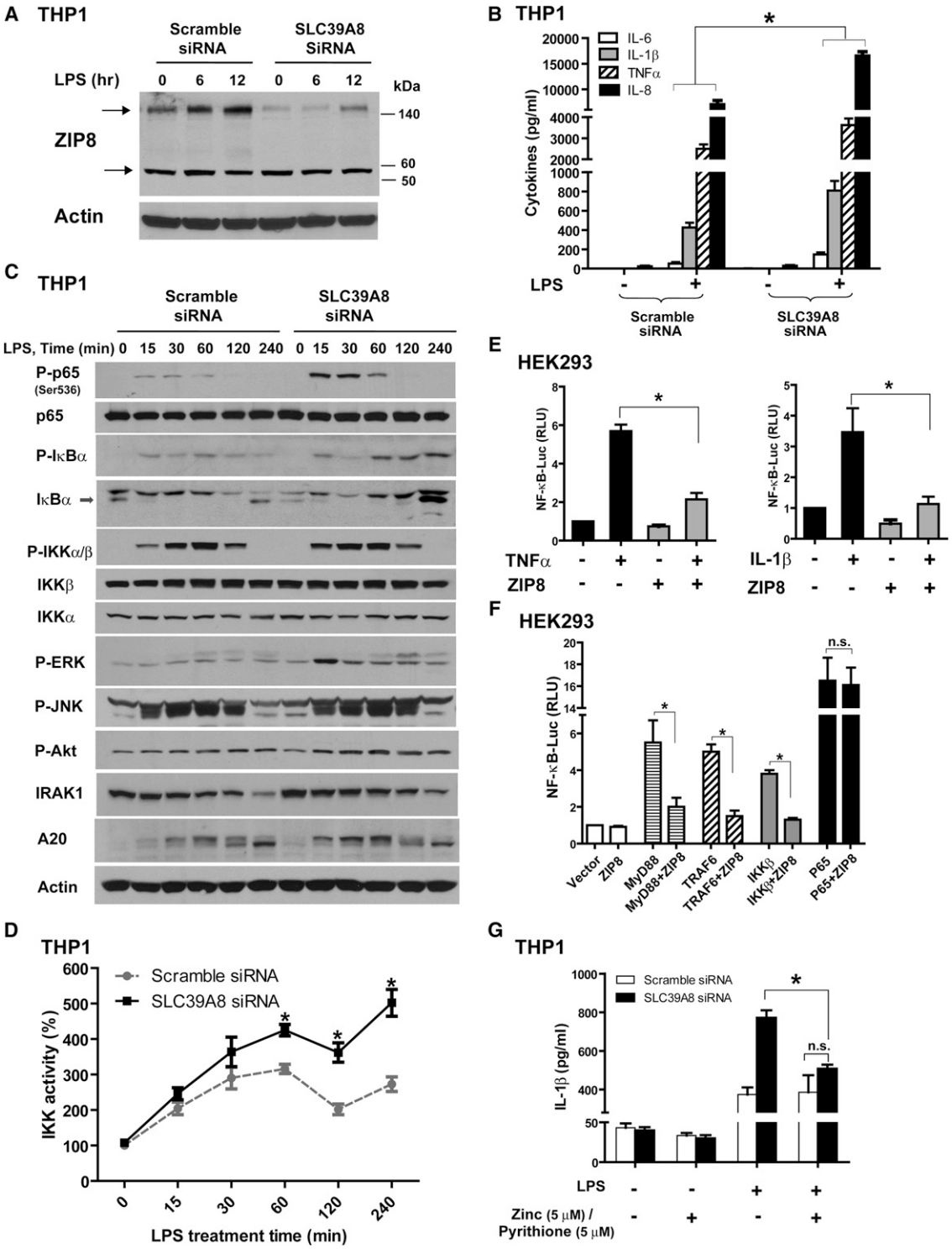

Figure 3. ZIP8 Modulates NF-κB Activity and the Inflammatory Response

(A and B) THP1 cells were transfected with either scrambled control or SLC39A8 siRNA for 3 days, followed by LPS (1 μg/ml × 6–12 hr) treatment. ZIP8 silencing was evaluated by western analysis. Cytokine levels in culture medium were determined by ELISA at 6 hr.

(C) Western blot analysis of signaling molecules in THP1 extracts following ZIP8 knockdown in combination with LPS treatment. P, phosphorylated.

(D) IKK activity was measured following IP of the IKK complex using an anti-iKKβ antibody.

(E) ZIP8 overexpression inhibits NF-κB activation induced by TNF-α or IL-1β. HEK293 cells were transfected with 3 × κB-luc and ZIP8 cDNA construct, followed by treatment with TNF-α (10 ng/ml) or IL-1β (20 ng/ml) for 24 hr.

(legend continued on next page)

Next, we observed that zinc directly binds to IKKβ (Figures 4D and S4D). Based on this, we then immunoprecipitated the IKKβ-associated protein complex from LPS-stimulated cultures and treated immunoprecipitates with the zinc-specific chelator TPEN to remove protein-bound zinc. TPEN chelation resulted in an increase of kinase activity, substantiating that zinc directly binds to IKK intracellularly and inhibits kinase activity (Figure S4E). Furthermore, using confocal microscopy, we observed that overexpressed dsRed-tagged IKKβ partially colocalized with intracellular labile zinc, further supporting a direct interaction between labile zinc and IKKβ within the cytosol (Figures 4E and S4F). The crystal structure of IKKβ (*Xenopus laevis*) has recently been reported by Xu et al. (2011). A human IKKβ protomer model was constructed based on homology modeling. Accordingly, we utilized a combination of in silico modeling and site-directed mutagenesis and revealed a zinc coordination site located at His 143. Strikingly, this coordination site resides within the C lobe of the kinase domain, which is critical for IKKβ catalytic activity and responsiveness to zinc-mediated inhibition (both human and mouse). The structural model predicts that the coordination site is comprised of the zinc-binding residues H137, H143, D204, and I141 (Figures 4F, 4G, and S4G–S4I). In contrast, mutation of H313 located within the ubiquitin-like domain (ULD), at a potential alternative zinc coordination site identified by our screening approach, did not alter zinc-mediated kinase inhibition, indicating that zinc does not impact kinase activity through a ULD-related interaction. Collectively, our findings reveal that ZIP8-mediated zinc transport is critical in attenuating NF-κB signaling through zinc-mediated inhibition of IKKβ kinase activity.

Zinc Deficiency Augments IKK Activity and the Inflammatory Response In Vivo

We recently reported that moderate zinc deficiency significantly increased systemic inflammation, tissue injury, and mortality in response to polymicrobial sepsis (Bao et al., 2010; Knoell et al., 2009). Having established that zinc inhibits NF-κB activation through IKKβ in vitro, we postulated that systemic zinc deficiency in mice would result in elevated inflammation that would correlate with insufficient control of IKK signaling. To test this hypothesis, adult mice were first administered a zinc-deficient diet for 3 weeks, followed by LPS injection or cecal ligation and puncture (CLP) treatment for 2 hr. Animals maintained on a zinc-deficient diet had a significant decrease in zinc levels in the serum, peripheral monocytes, and lung (Figures 5B and 5C) (Knoell et al., 2009). In response to CLP, zinc-deficient mice also exhibited a significant increase in serum proinflammatory cytokines (IL-6, KC, TNF-α, and MCP-1) and lung transcripts of NF-κB target genes when compared to their normal dietary counterparts, indicative of an elevation in NF-κB activation (Figures 5A and 5D). A significant increase of phosphorylated IκBα and IκBα degradation was also observed in the lung, consistent with increased IKKβ activity in the setting of zinc deficiency. ERK phosphorylation was also increased, whereas alterations in JNK phosphorylation were nominal (Figure 5E). Similar results were observed with LPS-exposed animals (Figures S5A–S5C) and an in vitro monocyte cell line model in which cells were grown in zinc-deficient medium (Figure S5D).

ZIP8 Is Upregulated and Correlates with Altered Zinc Metabolism In Vivo in Response to LPS and Sepsis

Based upon in vitro studies, we sought to determine whether the upregulation of ZIP8 could be recapitulated in vivo. A significant increase in ZIP8 mRNA and protein expression was observed in lung tissue in response to both CLP and endotoxin. Expression was localized to alveolar epithelia, upper-airway epithelia, and alveolar macrophages (Figures 6A–6C and S6A). *Slc39a8* expression did not change in the liver (data not shown); however, expression of *Slc39a14* (ZIP14), the closest homolog to *Slc39a8*, was upregulated in the liver (Figure S6B) (Liuzzi et al., 2005) but did not change in the lung (data not shown). At the same time, plasma zinc levels precipitously declined following LPS and CLP challenge, consistent with hypozincemia, in the absence of body zinc loss (Cousins and Leinart, 1988). In sharp contrast, zinc levels in the lung and liver increased. Also, consistent with human studies (Gaetke et al., 1997), plasma zinc levels began to recover toward baseline within 16 hr following LPS challenge. CLP resulted in persistent hypozincemia and accumulation of zinc in the lung and liver, presumably as a consequence of increased and prolonged systemic inflammation (Figures 6D, S6C, and S6D). Accordingly, an increase in tissue metallothionein was observed in the lung and liver in response to LPS and CLP treatment, which could result from zinc influx, inflammation, or both (Figures 6E and S6E). CLP also significantly increased both ZIP8 expression and intracellular zinc content in circulating monocytes (Figure 6F).

Slc39a8 Hypomorphic Mouse Fetal Fibroblasts Are More Responsive to Proinflammatory Cytokines

Obliteration of ZIP8 is embryo lethal precluding in vivo validation studies in *Slc39a8*-knockout mice. In lieu of this, we conducted studies in *Slc39a8* hypomorphic mice that harbor a $Slc39a8^{(neo)}$ allele that contains the neomycin-resistance gene (*neo*) in intron 3. Homozygous $Slc39a8^{(neo/neo)}$ mice have a significant reduction in ZIP8 mRNA and protein levels (>90%) and diminished zinc levels in vital tissues. Due to developmental defects, the $Slc39a8^{(neo/neo)}$ homozygotes die between GD18.5 and 48 hr postnatally (Gálvez-Peralta et al., 2012; Wang et al., 2011).

In order to examine the function of ZIP8, we generated mouse fetal fibroblasts (MFFs) from GD16.5 $Slc39a8^{(+/+)}$, $Slc39a8^{(+/neo)}$, and $Slc39a8^{(neo/neo)}$ mice. As expected, $Slc39a8^{(neo/neo)}$ MFFs had significantly diminished ZIP8 mRNA and protein levels compared to that in $Slc39a8^{(+/+)}$ and $Slc39a8^{(+/neo)}$ cells. Metallothionein (*Mt1*) expression was also decreased in $Slc39a8^{(neo/neo)}$

(F) HEK293 cells were transfected with MyD88, TRAF6, IKKβ, or p65 expression plasmids together with the ZIP8 cDNA and 3 × κB-luc constructs. Luciferase activity was measured 24 hr after transfection.

(G) Zinc addition normalized the extent of NF-κB activation in the cells subjected to ZIP8 knockdown. siRNA knockdown was performed, followed by LPS (1 μg/ml) treatment for 8 hr. Zinc (5 μM) and pyrithione (5 μM) were added 30 min prior to LPS.

Data are presented as mean ± SD. *$p < 0.05$. See also Figure S3.

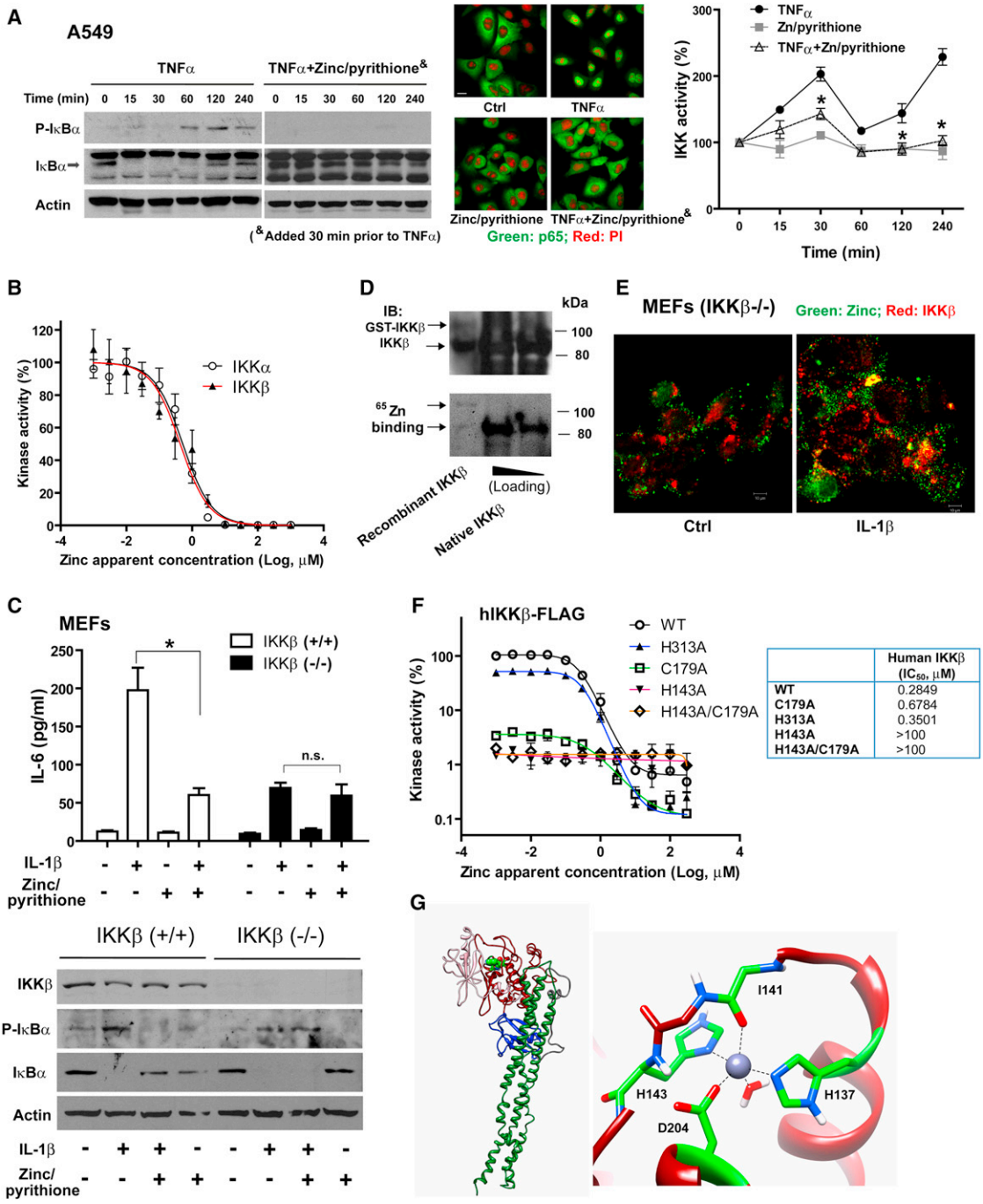

Figure 4. Zinc Inhibits NF-κB Activation through IKK

(A) Zinc (10 μM)/pyrithione (10 μM), added 30 min prior to TNF-α (10 ng/ml), inhibits NF-κB activation in A549 cells: western blot analysis (Figure S4A shows the entire blot); immunofluorescent staining of p65 at 30 min after TNF-α treatment (scale bar, 10 μm); IKK activity following IP of the IKK complex.

(B) Zinc inhibits human recombinant IKKα and IKKβ activity in a dose-dependent manner.

(C) Effect of zinc on IKKβ$^{(-/-)}$ MEFs. IKKβ$^{(-/-)}$ and IKKβ$^{(+/+)}$ MEFs were treated with zinc (10 μM)/pyrithione (2 μM) for 30 min, followed by IL-1β (200 ng/ml) treatment. IL-6 was measured in culture medium by ELISA at 6 hr. Western analysis was performed on samples at 30 min after IL-1β treatment.

(D) A ^{65}Zn-blotting assay was performed to evaluate zinc binding with IKKβ. Samples include recombinant IKKβ (cleaved and intact GST fusion) and native IKKβ that was immunoprecipitated from TNF-α-treated A549 cells.

(E) Confocal image analysis identified colocalization of reconstituted IKKβ-dsRed and zinc (FluoZin-3, green). IKKβ$^{(-/-)}$ MEFs were treated with IL-1β (100 ng/ml) for 4 hr. Figure S4F shows the images in multiple channels.

(F) Dose-response curves of zinc inhibition on IKKβ and corresponding mutants. The IC_{50} values are shown on the right.

(legend continued on next page)

cultures, most likely as a consequence of decreased intracellular zinc levels (Figure 7A). A time-dependent analysis of zinc content in culture medium revealed that *Slc39a8*$^{(neo/neo)}$ MFFs are impaired in their ability to uptake zinc in response to TNF-α (Figure 7B). We then examined the inflammatory response of MFFs to TNF-α and IL-1β. *Slc39a8*$^{(neo/neo)}$ MFFs produced more IL-6, compared with that in *Slc39a8*$^{(+/neo)}$ and *Slc39a8*$^{(+/+)}$ cells (Figures 7C and S7B), and consistently showed increased transcript levels of NF-κB-driven genes (Figures 7D, S7A, S7C, and S7D). Strikingly, the signaling events demonstrate that the presence of phosphorylated p65 and IκBα is elevated in *Slc39a8*$^{(neo/neo)}$ MFFs, in tandem with prolonged IκBα degradation. These findings are also consistent with elevated IKKβ activity, thereby further corroborating that ZIP8 negatively regulates NF-κB through IKKβ (Figure 7E).

DISCUSSION

Overwhelming bacterial infection quickly activates the innate immune response and triggers inflammation in order to enable host defense. The magnitude of the initial response must be agile, relative to the type and extent of infection, to facilitate pathogen removal, extinguish inflammation, and ultimately restore homeostasis. Indeed, in the words of Lewis Thomas, "Our arsenals for fighting off bacteria are so powerful, and involve so many different defense mechanisms, that we are in more danger from them than from the invaders" (Thomas, 1972). Consistent with his postulate, patients with sepsis typically do not succumb to the initial infection but rather succumb later to immune dysfunction, end-organ damage, and secondary infection. Mortality from sepsis and septic shock is strongly associated with overactivation of the initial inflammatory response (Abraham and Singer, 2007). Increased expression of NF-κB-driven cytokines, including TNF-α, IL-1β, and IL-6, is associated with increased risk for vital organ failure and a worse prognosis (Hotchkiss and Karl, 2003), but it is still not known why immune imbalance occurs.

Multiple negative feedback pathways have evolved to control the extent of innate immune activation (Ruland, 2011). Herein, we report a unique negative feedback regulator, ZIP8, that directly couples zinc metabolism to the regulation of innate immunity. ZIP8 shares a similar feature with other established NF-κB-negative feedback regulators, including IκBα (Chiao et al., 1994) and A20 (Boone et al., 2004), in that its expression requires activation by the very pathway it controls; however, ZIP8 is unique in that its function is coupled to the importation of zinc. Furthermore, ZIP8 functions by guiding zinc into the cytosol to inhibit IKKβ, thereby regulating immune balance. Zinc directly binds to a coordination site in IKKβ that includes H143 within the kinase domain. Because H143 together with D145 and Mg^{2+} are known to coordinate ATP binding, we predict that zinc interaction with H143 will result in a rotameric switch that weakens ATP binding, thereby reducing or inactivating IKKβ enzyme activity, although this remains to be established (Figure 4G). IKKβ also serves as a critical switch for activating the ERK signaling pathway (Banerjee and Gerondakis, 2007). Consistent with this, we observed that ZIP8-mediated zinc transport inhibited ERK signaling. The function of zinc in concert with ZIP8 on NF-κB is conserved in different cell types, including monocytes, macrophages, and lung epithelial cells. Consistent with this, loss of the zinc exporter *Slc30a5* (Znt5) in mast cells resulted in increased labile zinc and suppressed NF-κB signaling in response to FcεRI stimulators (Nishida et al., 2009). However, it is important to recognize that zinc function and trafficking are highly dependent on the cell type within the context of cell activation. For example, TLR4 stimulation in dendritic cells decreases cytosolic-free zinc through the suppression of ZIP6 (Kitamura et al., 2006). T cell ($CD3^+$) activation upregulates ZIP8, which promotes labile zinc release from the lysosome and enhances IFN-γ production (Aydemir et al., 2009). TCR activation in $CD4^+$ T cells induces zinc influx through ZIP6, resulting in augmentation of TCR signaling (Yu et al., 2011). These important findings underscore the complexity of zinc metabolism relative to immune function.

Humans and bacteria, in many respects, are engaged in a "tug of war" at the host-microbial interface and compete for vital resources to maintain essential biological functions (Kehl-Fie and Skaar, 2010). We speculate that zinc, typically abundant within the extracellular milieu, is a vital commodity at the onset of infection and that ZIP8 plays a vital role to uptake zinc into host cells thereby providing a competitive advantage. Zinc metabolism and turnover in humans are relatively high, with approximately 1% of total body zinc content replenished daily by the diet (King et al., 2000). In cells, a labile zinc pool is rapidly exchangeable and altered in response to zinc conditions as well as to extracellular stimuli. Labile zinc regulates signaling, through both kinases and phosphatases, and its levels are maintained by zinc transporters (Haase and Rink, 2007). Recent elucidation of ZIP protein structure has revealed that zinc transport is a nonsaturable and electrogenic process consistent with features of a zinc-permeable channel (Lin et al., 2010), a model distinct from conventional ATP or voltage-gated transport, indicating that expression of ZIPs is coupled to functional control. Moreover, as we reveal, ZIP8 is directly regulated by NF-κB at the transcriptional level, making it unique and highly specialized to allow the rapid sequestration of zinc in response to infection. Similar to ZIP8, ZIP14 is regulated by IL-6-dependent signaling in the liver (Liuzzi et al., 2005). Phylogenetic analysis of SLC39 family proteins reveals that ZIP8 and ZIP14 are related and distinct from the other 12 ZIPs (Girijashanker et al., 2008). This is intriguing when taking into account that both genes emerged in land animals from a single gene in sea animals approximately 420 million years ago. This evolutionary divergence supports the notion that specialized zinc transporter function(s) may have evolved as a consequence of new environmental pressures. As driven in part by ZIP8 and ZIP14, hypozincemia is a well-characterized phenomenon that occurs in response to systemic

(G) Model of zinc coordination in the kinase domain of human IKKβ. Left view is the computationally derived model of the human IKKβ protomer, including the N and C lobe of the kinase domain (pink and red, respectively), the ULD (blue), and the scaffold/dimerization domain (dark green). Highlighted in bright green is the zinc-binding site in the C lobe of the kinase domain. On the right is a magnified view of the zinc-binding site and contributing binding residues.
Data are presented as mean ± SD. *$p < 0.05$. See also Figure S4.

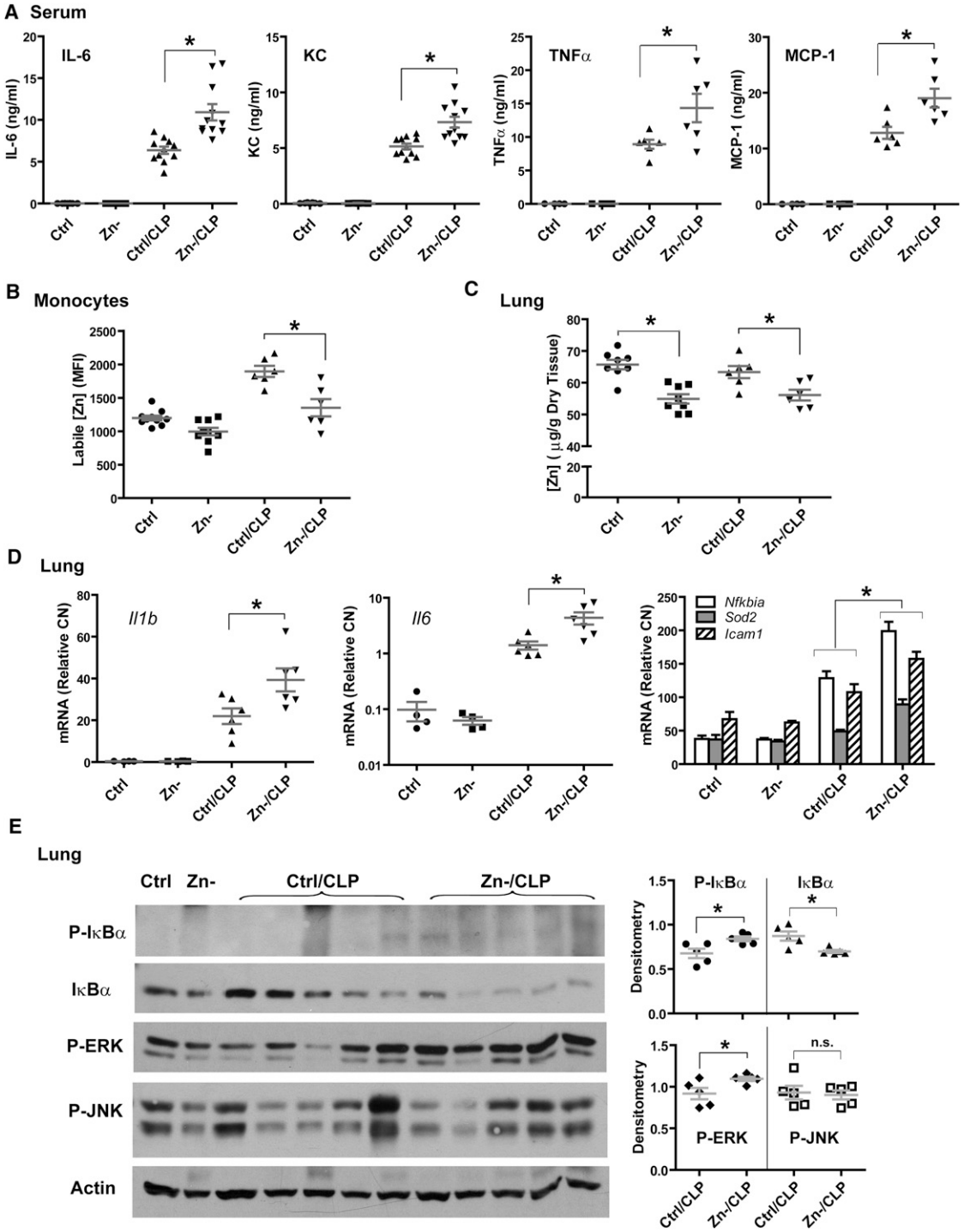

Figure 5. Systemic Zinc Deficiency Increases the Proinflammatory Response to Sepsis

(A) Cytokine analysis of serum obtained from mice that were maintained on zinc-deficient or corresponding control diet for 3 weeks, followed by CLP. Samples were obtained 2 hr after CLP. Zn, zinc; Zn−, zinc deficient; Ctrl/CLP: control (normal) diet plus CLP; Zn−/CLP, zinc-deficient diet plus CLP.

(B) Labile zinc levels in peripheral blood monocytes at 2 hr after CLP. Figure 6F describes the methodology.

(C) Total zinc levels in the lung at 2 hr after CLP, as measured by AAS.

(D) Gene expression analysis of NF-κB target genes in mouse lung tissues.

(E) Total proteins were extracted from lung and subjected to western analysis. Densitometry is presented as a histogram to the right.

Data are presented as mean ± SEM. *$p < 0.05$. See also Figure S5.

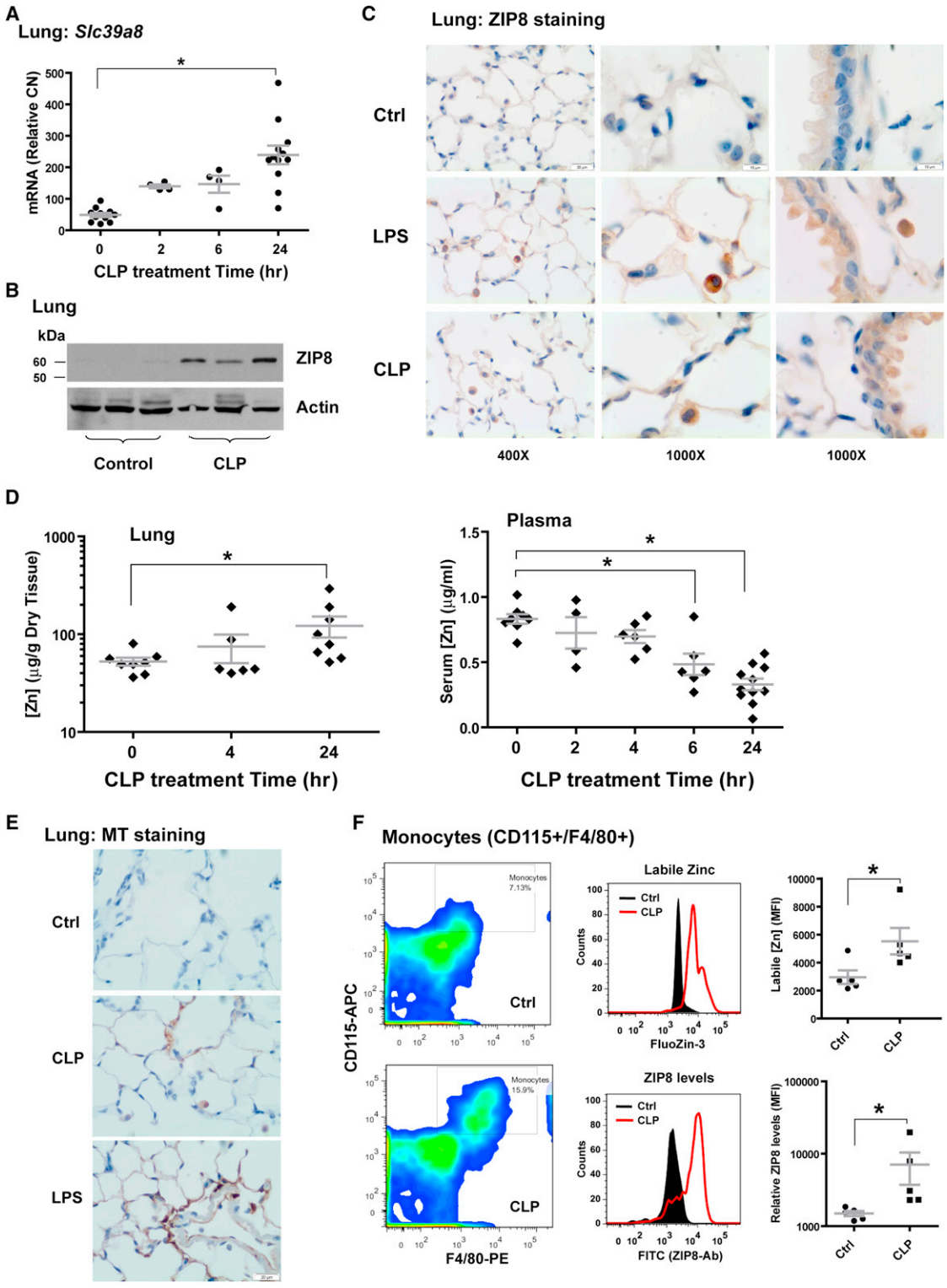

Figure 6. Endotoxin or Sepsis Induces *Slc39a8* Expression Resulting in Increased Zinc Levels in Lung and Monocytes

(A) *Slc39a8* expression was induced in mouse lung following CLP treatment.

(B) Western blot analysis shows the induction of ZIP8 protein in whole-lung homogenates 24 hr after CLP.

(C) Immunostaining shows that ZIP8 expression is increased at 24 hr following LPS or CLP treatment in alveolar epithelia, upper-airway epithelia, and alveolar macrophages (scale bars, 20 μm for 400× and 10 μm for 1,000× magnification).

(legend continued on next page)

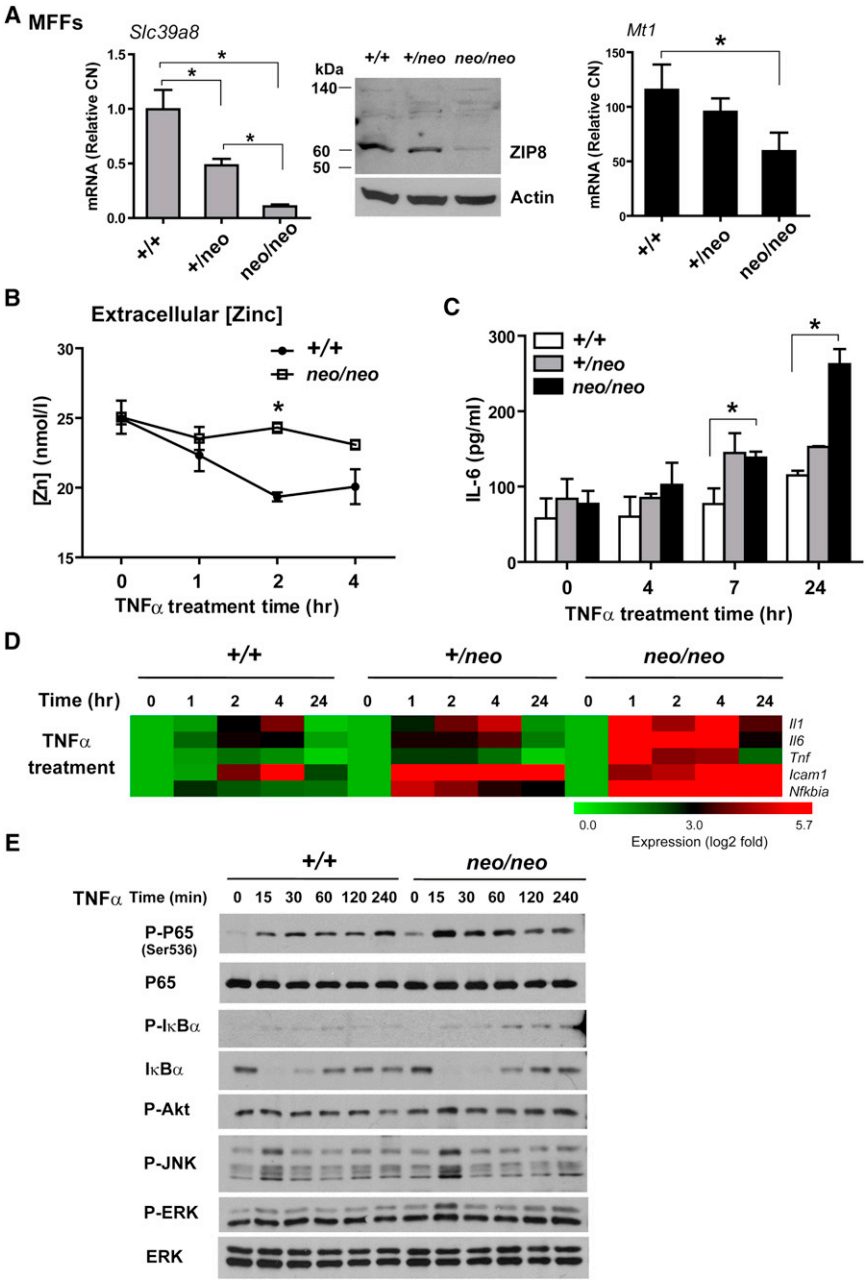

Figure 7. *Slc39a8* Hypomorphic MFFs Have an Elevated Proinflammatory Response to TNF-α

(A) Real-time PCR quantified the mRNA levels of ZIP8 and MT1 in *Slc39a8*$^{(+/+)}$, *Slc39a8*$^{(+/neo)}$, and *Slc39a8*$^{(neo/neo)}$ primary MFFs cultures. Western analysis shows ZIP8 protein levels.

(B) Total zinc levels in culture medium were determined by AAS.

(C) *Slc39a8*$^{(+/+)}$, *Slc39a8*$^{(+/neo)}$, and *Slc39a8*$^{(neo/neo)}$ MFFs were treated with mouse TNF-α (50 ng/ml) for the indicated time. IL-6 levels were measured in the culture supernatants.

(D) Analysis of proinflammatory gene expression profiles in *Slc39a8*$^{(+/+)}$, *Slc39a8*$^{(+/neo)}$, and *Slc39a8*$^{(neo/neo)}$ MFFs that were treated with TNF-α for the indicated time points. Data are presented as a representative heatmap following normalization to untreated group. Gene designation is to the right of each row.

(E) Western blot analysis of signaling pathways in *Slc39a8*$^{(+/+)}$ and *Slc39a8*$^{(neo/neo)}$ MFFs treated with TNF-α.

Data are presented as mean ± SD. *p < 0.05. See also Figure S7.

infection and inflammation (Cousins and Leinart, 1988; Gaetke et al., 1997; Sobocinski et al., 1978). Based on our findings that correlate with in vivo observations, we propose that ZIP8 and ZIP14 are unique zinc transporters that are rapidly induced in a tissue-specific manner, thereby channeling zinc to fundamentally important intracellular checkpoints that help to coordinate and balance host defense.

Zinc deficiency is a significant health care problem (Hambidge and Krebs, 2007) and a leading cause of infections including pneumonia, diarrhea, and malaria (Caulfield et al., 2004). Rapid changes in zinc metabolism that lead to hypozincemia are common in critically ill patients. Septic shock nonsurvivors have lower serum zinc levels, compared with survivors who are able to recover from hypozincemia (Wong et al., 2007). In adult septic subjects, lower plasma zinc levels correlated with higher ZIP8 expression levels in monocytes, higher cytokine levels, and increased organ damage within the first 24 hr following ICU admission (Besecker et al., 2011). Based upon these observations, it is plausible that prolonged hypozincemia and elevated ZIP8 expression in monocytes might be useful prognostically as a guide for zinc supplementation in patients with sepsis. Zinc supplementation has been shown to prevent the incidence of serious infections in children (Brooks et al., 2005). We also

(D) Time-lapse analysis of zinc levels in serum and lung tissue, following CLP exposure.

(E) Metallothionein (MT) staining in the lung 24 hr after LPS or CLP (scale bar, 20 μm).

(F) Mouse peripheral leukocytes were stained with CD115-APC and F4/80-Pacific Blue, along with FluoZin-3 or ZIP8 antibody and FITC-secondary conjugate. Monocytes were selected as CD115+/F4/80+ cells, followed by histogram analysis of FluoZin-3 or FITC-positive cells within this population. The relative levels of zinc or ZIP8 were compared, based on MFI.

Data are presented as mean ± SEM. *p < 0.05. See also Figure S6.

observed that zinc supplementation significantly improves survival in an animal model of combined zinc deficiency and sepsis (Knoell et al., 2009). Further investigation is needed to understand the complexity of zinc metabolism throughout the entire course of sepsis before we are able to determine the impact of zinc supplementation on patients with sepsis. Accurate biomarkers that are predictive of zinc status will also be required because plasma zinc levels are a poor indicator in the setting of inflammation.

In conclusion, we report that the zinc transporter SLC39A8 is a negative regulator of the NF-κB signaling pathway through zinc-mediated suppression of IKK activity in monocytes, macrophages, and lung epithelia. In vivo, ZIP8 expression is induced following innate immune activation and correlates with intracellular zinc sequestration. We contend that these findings bridge a fundamental gap in our understanding of how zinc metabolism, or deficits therein, may critically influence the initial host response to infection. In addition, they provide a framework for understanding how inadequate zinc consumption can increase risk of immune dysfunction, thereby compromising the host's capability to battle pathogens at the front line of defense.

EXPERIMENTAL PROCEDURES

Animal Studies

C57BL/6 mice (The Jackson Laboratory) were either injected (5 μg/g body weight) intraperitoneally (i.p.) with LPS (*Escherichia coli* serotype 055:B5; Sigma-Aldrich) or treated with CLP. To establish systemic zinc-deficiency model, mice were randomly placed on a zinc-deficient diet (0.5–1.5 ppm zinc) or a matched control diet (50.5–51.5 ppm zinc) for 3 weeks (Knoell et al., 2009). All animal studies were conducted in accordance with the terms and conditions of prior approval as set forth by The Ohio State University Institutional Animal Care and Use Committee.

Real-Time PCR

Quantitative PCR was performed using SYBR Green reagent (Applied Biosystems). Relative copy numbers (RCNs) of selected genes were normalized to the expression of housekeeping genes (GAPDH or cyclophilin), then calculated with the following equation: $RCN = 2^{-\Delta Ct} \times 100$, where ΔCt is the $Ct_{(target)} - Ct_{(reference)}$. PCR primers are listed in Table S1.

Promoter Cloning and Luciferase Assay

SLC39A8 luciferase reporter constructs were generated from human genomic DNA using PCR amplification of an approximately 2,000 bp promoter fragment, followed by insertion into pGL3 vector. Deletion constructs were generated using a PCR-based subcloning strategy. Sequence analysis confirmed the fidelity of all the constructs. Luciferase assay was performed with Dual-Glo system (Promega). Cloning primers are listed in Table S1.

Western Blot, Immunoprecipitation, and Kinase Assay

Standard western blot and immunoprecipitation (IP) were performed. Kinase assay was performed using the HTScan Kinase Assay Kit, with IκBα (Ser32) peptide as the specific substrate (Cell Signaling Technology).

^{65}Zinc-Blotting Assay

Protein samples were resolved by SDS-PAGE and transferred to a PVDF membrane. Immunoblotting (IB) was first conducted using anti-iKKβ antibody, followed by intense stripping. Proteins on PVDF filter were renatured and incubated with 100 μCi of $^{65}ZnCl_2$. Autoradiography was then performed.

Zinc Measurement by Atomic Absorption Spectroscopy or Inductively Coupled Plasma Optical-Emission Spectrometry

Solid tissues were dried, weighted, and digested in 1 ml mixed acid solution (nitric acid:perchloric acid [1:2]) at 80°C for 4–6 hr. Liquid samples were digested with nitric acid (1%) for overnight. Samples were subjected to atomic absorption spectroscopy (AAS) (AAnalyst 400; PerkinElmer) or a Vista-PRO inductively coupled plasma optical-emission spectrometry (ICP-OES) (Varian).

Statistics

Data are representative of three independent experiments (mean ± SD or SEM). Statistical comparisons among multiple groups were performed using one-way ANOVA with Tukey's or Dunnett's post hoc test. Comparison among four groups with two factors was performed using 2 × 2 factorial ANOVA. Pairs of treatment groups were compared using two-tailed unpaired Student's t test. Significance was assumed at a p value of less than 0.05 (*$p < 0.05$; n.s., not significantly different).

SUPPLEMENTAL INFORMATION

Supplemental Information includes seven figures, one table, and Extended Experimental Procedures and can be found with this article online at http://dx.doi.org/10.1016/j.celrep.2013.01.009.

LICENSING INFORMATION

This is an open-access article distributed under the terms of the Creative Commons Attribution-NonCommercial-No Derivative Works License, which permits non-commercial use, distribution, and reproduction in any medium, provided the original author and source are credited.

ACKNOWLEDGMENTS

Dr. Denis Guttridge (The Ohio State University) provided the p65, p50, and IκBα-SR plasmids. Drs. Michael Karin (University of California, San Diego) and Ying Xia (University of Cincinnati) provided IKKβ and NEMO knockout MEFs. Technical support was provided by Catherine Powell, Dara Burris, Chuan Yu, David Vera, and Bryan Lee. This work was supported by Lifeline of Ohio Tissue Procurement Agency and the National Institutes of Health (HL R01 HL086981-01 to D.L.K., T32 ES016646 to M.G.-P., and P30 ES06096 and R01 ES010416 to D.W.N.).

Received: July 26, 2012
Revised: November 28, 2012
Accepted: January 14, 2013
Published: February 7, 2013

REFERENCES

Abraham, E., and Singer, M. (2007). Mechanisms of sepsis-induced organ dysfunction. Crit. Care Med. *35*, 2408–2416.

Aiba, I., Hossain, A., and Kuo, M.T. (2008). Elevated GSH level increases cadmium resistance through down-regulation of Sp1-dependent expression of the cadmium transporter ZIP8. Mol. Pharmacol. *74*, 823–833.

Angus, D.C., Linde-Zwirble, W.T., Lidicker, J., Clermont, G., Carcillo, J., and Pinsky, M.R. (2001). Epidemiology of severe sepsis in the United States: analysis of incidence, outcome, and associated costs of care. Crit. Care Med. *29*, 1303–1310.

Aydemir, T.B., Liuzzi, J.P., McClellan, S., and Cousins, R.J. (2009). Zinc transporter ZIP8 (SLC39A8) and zinc influence IFN-gamma expression in activated human T cells. J. Leukoc. Biol. *86*, 337–348.

Banerjee, A., and Gerondakis, S. (2007). Coordinating TLR-activated signaling pathways in cells of the immune system. Immunol. Cell Biol. *85*, 420–424.

Banerjee, A., Gugasyan, R., McMahon, M., and Gerondakis, S. (2006). Diverse Toll-like receptors utilize Tpl2 to activate extracellular signal-regulated kinase (ERK) in hemopoietic cells. Proc. Natl. Acad. Sci. USA *103*, 3274–3279.

Bao, S., Liu, M.J., Lee, B., Besecker, B., Lai, J.P., Guttridge, D.C., and Knoell, D.L. (2010). Zinc modulates the innate immune response in vivo to polymicrobial sepsis through regulation of NF-kappaB. Am. J. Physiol. Lung Cell. Mol. Physiol. *298*, L744–L754.

Begum, N.A., Kobayashi, M., Moriwaki, Y., Matsumoto, M., Toyoshima, K., and Seya, T. (2002). Mycobacterium bovis BCG cell wall and lipopolysaccharide induce a novel gene, BIGM103, encoding a 7-TM protein: identification of a new protein family having Zn-transporter and Zn-metalloprotease signatures. Genomics *80*, 630–645.

Besecker, B., Bao, S., Bohacova, B., Papp, A., Sadee, W., and Knoell, D.L. (2008). The human zinc transporter SLC39A8 (Zip8) is critical in zinc-mediated cytoprotection in lung epithelia. Am. J. Physiol. Lung Cell. Mol. Physiol. *294*, L1127–L1136.

Besecker, B.Y., Exline, M.C., Hollyfield, J., Phillips, G., Disilvestro, R.A., Wewers, M.D., and Knoell, D.L. (2011). A comparison of zinc metabolism, inflammation, and disease severity in critically ill infected and noninfected adults early after intensive care unit admission. Am. J. Clin. Nutr. *93*, 1356–1364.

Boone, D.L., Turer, E.E., Lee, E.G., Ahmad, R.C., Wheeler, M.T., Tsui, C., Hurley, P., Chien, M., Chai, S., Hitotsumatsu, O., et al. (2004). The ubiquitin-modifying enzyme A20 is required for termination of Toll-like receptor responses. Nat. Immunol. *5*, 1052–1060.

Brooks, W.A., Santosham, M., Naheed, A., Goswami, D., Wahed, M.A., Diener-West, M., Faruque, A.S., and Black, R.E. (2005). Effect of weekly zinc supplements on incidence of pneumonia and diarrhoea in children younger than 2 years in an urban, low-income population in Bangladesh: randomised controlled trial. Lancet *366*, 999–1004.

Burns, K., Janssens, S., Brissoni, B., Olivos, N., Beyaert, R., and Tschopp, J. (2003). Inhibition of interleukin 1 receptor/Toll-like receptor signaling through the alternatively spliced, short form of MyD88 is due to its failure to recruit IRAK-4. J. Exp. Med. *197*, 263–268.

Caulfield, L.E., de Onis, M., Blössner, M., and Black, R.E. (2004). Undernutrition as an underlying cause of child deaths associated with diarrhea, pneumonia, malaria, and measles. Am. J. Clin. Nutr. *80*, 193–198.

Chiao, P.J., Miyamoto, S., and Verma, I.M. (1994). Autoregulation of I kappa B alpha activity. Proc. Natl. Acad. Sci. USA *91*, 28–32.

Cousins, R.J., and Leinart, A.S. (1988). Tissue-specific regulation of zinc metabolism and metallothionein genes by interleukin 1. FASEB J. *2*, 2884–2890.

Cui, J., Zhu, L., Xia, X., Wang, H.Y., Legras, X., Hong, J., Ji, J., Shen, P., Zheng, S., Chen, Z.J., and Wang, R.F. (2010). NLRC5 negatively regulates the NF-kappaB and type I interferon signaling pathways. Cell *141*, 483–496.

Gaetke, L.M., McClain, C.J., Talwalkar, R.T., and Shedlofsky, S.I. (1997). Effects of endotoxin on zinc metabolism in human volunteers. Am. J. Physiol. *272*, E952–E956.

Gálvez-Peralta, M., He, L., Jorge-Nebert, L.F., Wang, B., Miller, M.L., Eppert, B.L., Afton, S., and Nebert, D.W. (2012). ZIP8 zinc transporter: indispensable role for both multiple-organ organogenesis and hematopoiesis in utero. PLoS One *7*, e36055.

Girijashanker, K., He, L., Soleimani, M., Reed, J.M., Li, H., Liu, Z., Wang, B., Dalton, T.P., and Nebert, D.W. (2008). Slc39a14 gene encodes ZIP14, a metal/bicarbonate symporter: similarities to the ZIP8 transporter. Mol. Pharmacol. *73*, 1413–1423.

Haase, H., and Rink, L. (2007). Signal transduction in monocytes: the role of zinc ions. Biometals *20*, 579–585.

Haase, H., and Rink, L. (2009). Functional significance of zinc-related signaling pathways in immune cells. Annu. Rev. Nutr. *29*, 133–152.

Hambidge, K.M., and Krebs, N.F. (2007). Zinc deficiency: a special challenge. J. Nutr. *137*, 1101–1105.

Hayden, M.S., and Ghosh, S. (2008). Shared principles in NF-kappaB signaling. Cell *132*, 344–362.

Hotchkiss, R.S., and Karl, I.E. (2003). The pathophysiology and treatment of sepsis. N. Engl. J. Med. *348*, 138–150.

Jeon, K.I., Jeong, J.Y., and Jue, D.M. (2000). Thiol-reactive metal compounds inhibit NF-kappa B activation by blocking I kappa B kinase. J. Immunol. *164*, 5981–5989.

Johnson, G.L., and Lapadat, R. (2002). Mitogen-activated protein kinase pathways mediated by ERK, JNK, and p38 protein kinases. Science *298*, 1911–1912.

Kawai, T., and Akira, S. (2010). The role of pattern-recognition receptors in innate immunity: update on Toll-like receptors. Nat. Immunol. *11*, 373–384.

Kehl-Fie, T.E., and Skaar, E.P. (2010). Nutritional immunity beyond iron: a role for manganese and zinc. Curr. Opin. Chem. Biol. *14*, 218–224.

King, J.C., Shames, D.M., and Woodhouse, L.R. (2000). Zinc homeostasis in humans. J. Nutr. *130*(5S, Suppl), 1360S–1366S.

Kitamura, H., Morikawa, H., Kamon, H., Iguchi, M., Hojyo, S., Fukada, T., Yamashita, S., Kaisho, T., Akira, S., Murakami, M., and Hirano, T. (2006). Toll-like receptor-mediated regulation of zinc homeostasis influences dendritic cell function. Nat. Immunol. *7*, 971–977.

Knoell, D.L., Julian, M.W., Bao, S., Besecker, B., Macre, J.E., Leikauf, G.D., DiSilvestro, R.A., and Crouser, E.D. (2009). Zinc deficiency increases organ damage and mortality in a murine model of polymicrobial sepsis. Crit. Care Med. *37*, 1380–1388.

Kobayashi, K., Hernandez, L.D., Galán, J.E., Janeway, C.A., Jr., Medzhitov, R., and Flavell, R.A. (2002). IRAK-M is a negative regulator of Toll-like receptor signaling. Cell *110*, 191–202.

Li, Q., Van Antwerp, D., Mercurio, F., Lee, K.F., and Verma, I.M. (1999). Severe liver degeneration in mice lacking the IkappaB kinase 2 gene. Science *284*, 321–325.

Lichten, L.A., and Cousins, R.J. (2009). Mammalian zinc transporters: nutritional and physiologic regulation. Annu. Rev. Nutr. *29*, 153–176.

Liew, F.Y., Xu, D., Brint, E.K., and O'Neill, L.A. (2005). Negative regulation of toll-like receptor-mediated immune responses. Nat. Rev. Immunol. *5*, 446–458.

Lin, W., Chai, J., Love, J., and Fu, D. (2010). Selective electrodiffusion of zinc ions in a Zrt-, Irt-like protein, ZIPB. J. Biol. Chem. *285*, 39013–39020.

Liuzzi, J.P., Lichten, L.A., Rivera, S., Blanchard, R.K., Aydemir, T.B., Knutson, M.D., Ganz, T., and Cousins, R.J. (2005). Interleukin-6 regulates the zinc transporter Zip14 in liver and contributes to the hypozincemia of the acute-phase response. Proc. Natl. Acad. Sci. USA *102*, 6843–6848.

Martin, G.S., Mannino, D.M., Eaton, S., and Moss, M. (2003). The epidemiology of sepsis in the United States from 1979 through 2000. N. Engl. J. Med. *348*, 1546–1554.

Nishida, K., Hasegawa, A., Nakae, S., Oboki, K., Saito, H., Yamasaki, S., and Hirano, T. (2009). Zinc transporter Znt5/Slc30a5 is required for the mast cell-mediated delayed-type allergic reaction but not the immediate-type reaction. J. Exp. Med. *206*, 1351–1364.

Parrillo, J.E. (1993). Pathogenetic mechanisms of septic shock. N. Engl. J. Med. *328*, 1471–1477.

Prasad, A.S., Beck, F.W., Bao, B., Fitzgerald, J.T., Snell, D.C., Steinberg, J.D., and Cardozo, L.J. (2007). Zinc supplementation decreases incidence of infections in the elderly: effect of zinc on generation of cytokines and oxidative stress. Am. J. Clin. Nutr. *85*, 837–844.

Rink, L., and Haase, H. (2007). Zinc homeostasis and immunity. Trends Immunol. *28*, 1–4.

Rudolph, D., Yeh, W.C., Wakeham, A., Rudolph, B., Nallainathan, D., Potter, J., Elia, A.J., and Mak, T.W. (2000). Severe liver degeneration and lack of NF-kappaB activation in NEMO/IKKgamma-deficient mice. Genes Dev. *14*, 854–862.

Ruland, J. (2011). Return to homeostasis: downregulation of NF-κB responses. Nat. Immunol. *12*, 709–714.

Sobocinski, P.Z., Canterbury, W.J., Jr., Mapes, C.A., and Dinterman, R.E. (1978). Involvement of hepatic metallothioneins in hypozincemia associated with bacterial infection. Am. J. Physiol. *234*, E399–E406.

Takeuchi, O., and Akira, S. (2010). Pattern recognition receptors and inflammation. Cell *140*, 805–820.

Thomas, L. (1972). Germs. N. Engl. J. Med. *287*, 553–555.

Wang, B., He, L., Dong, H., Dalton, T.P., and Nebert, D.W. (2011). Generation of a Slc39a8 hypomorph mouse: markedly decreased ZIP8 $Zn^{2+}/(HCO_3^-)_2$ transporter expression. Biochem. Biophys. Res. Commun. *410*, 289–294.

Warren, H.S. (1997). Strategies for the treatment of sepsis. N. Engl. J. Med. *336*, 952–953.

Waterfield, M., Jin, W., Reiley, W., Zhang, M., and Sun, S.C. (2004). IkappaB kinase is an essential component of the Tpl2 signaling pathway. Mol. Cell. Biol. *24*, 6040–6048.

Wong, H.R., Shanley, T.P., Sakthivel, B., Cvijanovich, N., Lin, R., Allen, G.L., Thomas, N.J., Doctor, A., Kalyanaraman, M., Tofil, N.M., et al.; Genomics of Pediatric SIRS/Septic Shock Investigators (2007). Genome-level expression profiles in pediatric septic shock indicate a role for altered zinc homeostasis in poor outcome. Physiol. Genomics *30*, 146–155.

Xu, G., Lo, Y.C., Li, Q., Napolitano, G., Wu, X., Jiang, X., Dreano, M., Karin, M., and Wu, H. (2011). Crystal structure of inhibitor of κB kinase β. Nature *472*, 325–330.

Yu, M., Lee, W.W., Tomar, D., Pryshchep, S., Czesnikiewicz-Guzik, M., Lamar, D.L., Li, G., Singh, K., Tian, L., Weyand, C.M., and Goronzy, J.J. (2011). Regulation of T cell receptor signaling by activation-induced zinc influx. J. Exp. Med. *208*, 775–785.